PHILOSOPHICAL TRANSACTIONS OF THE ROYAL SOCIETY A MATHEMATICAL, PHYSICAL & ENGINEERING SCIENCES

Phonon Spectroscopy and Surface Reconstruction [and Discussion]

H. Ibach, J. E. Muller, Talat S. Rahman and M. W. Roberts

Phil. Trans. R. Soc. Lond. A 1986 **318**, 163-178
doi: 10.1098/rsta.1986.0069

Phil. Trans. R. Soc. Lond. A **318**, 163–178 (1986) [163]
Printed in Great Britain

Phonon spectroscopy and surface reconstruction

By H. Ibach,[1] J. E. Müller[2] and Talat S. Rahman[3]

[1] *Institut für Grenzflächenforschung und Vakuumphysik, Kernforschungsanlage Jülich, Postfach* 1913, *D*-5170 *Jülich, F.R.G.*

[2] *Projekt Spallations-Neutronenquelle, Kernforschungsanlage Jülich, Postfach* 1913, *D*-5170 *Jülich, F.R.G.*

[3] *Department of Physics, Cardwell Hall, Kansas State University, Manhattan, Kansas* 66506, *U.S.A.*

The nature of the recently discovered reconstruction of the Ni(100) surface under the influence of a $c(2\times2)$ carbon overlayer is investigated. A lattice dynamical analysis of the phonon dispersion of Ni(100) surfaces covered with $c(2\times2)$ overlayers of sulphur and oxygen suggests that the second derivative of the pair potential between the first- and second-layer nickel atoms is very sensitive to the adsorbed species. It is shown that the observed reconstruction pattern with the carbon overlayer follows naturally from the assumption that the second derivative becomes zero or negative for the unreconstructed atom positions. The effect could be an indication of internal strains caused by the adsorbate. Total energy calculations using the Hohenberg–Kohn–Sham density functional scheme on an Al_9-cluster indeed provide an indication for such strains. A detailed analysis shows further that the observed reconstruction may also result from an adsorbate-induced compression within the first layer.

1. Introduction

Since the original work of Farnsworth *et al.* (1958), reconstruction has been observed with many surfaces (Somorjai 1981). Some materials, like Si, Ge, GaAs, W, Mo, Pt, bear reconstructed surfaces even when clean, while other surfaces reconstruct with the adsorption of adatoms. In considering theoretical models for the reconstruction mechanism it is useful to distinguish between the class of reconstructions where the surface atoms are only moderately shifted from their bulk positions and the class of reconstructions where a major rearrangement of surface and subsurface atoms is involved. Historically, both types of models have frequently been advocated for the same surface. For the first class of models with only small displacements of atoms from their bulk positions the concept of a soft-phonon-driven reconstruction has been proposed (Cunningham & Trollinger 1978; Fasolino *et al.* 1980). The soft-phonon concept is able to establish a connection between a reconstruction pattern, as observed experimentally, and the inter-atomic forces. This obviously provides a useful step towards a more complete understanding of the origin of the reconstruction and lays the ground work for a more thorough analysis of the problem, which must involve consideration of the electronic structure of the material near the surface.

In this paper we discuss the results of a systematic experimental study of the phonon dispersion of Ni(100) surfaces covered with $c(2\times2)$ overlayers of sulphur, oxygen and carbon, together with a lattice dynamical analysis of the data. The analysis shows that with the sulphur overlayer nothing noteworthy happens to the coupling between the nickel atoms in the first and the second layer and a fit to the dispersion data can be obtained by assuming this force constant

to be at its clean-surface value. On the other hand, for the oxygen overlayer there is a relaxation of the interlayer distance and also a softening of the interlayer force constant. If one assumes that this trend continues such that the same force constant becomes zero or negative with the carbon overlayer, the surface should reconstruct. The lattice dynamical analysis of the resulting reconstruction pattern allows us to choose between the two proposed models for the experimentally observed reconstruction of the Ni(100) surface.

We next study the principle of an adsorbate-induced reconstruction in a total energy calculation that uses the Hohenberg–Kohn–Sham density functional scheme. For simplicity we have employed an Al_9-cluster of appropriate symmetry to simulate the (100) surface and one layer underneath. It is shown that the apparent softening of the force constant could be understood by a repulsion between the adsorbate and second-layer substrate atoms, which would cause an internal strain. This strain enlarges the distance between the first- and second-layer substrate atoms and thus reduces the second derivative of the pair potential between these substrate atoms to become eventually negative. The quantitative result on the Al_9-cluster, however, suggests an alternative picture, namely that carbon introduces a compression within the first layer. It is shown that this compression can also cause the observed reconstruction pattern.

2. Phonon dispersion curves of clean and $c(2\times2)$ covered f.c.c.(100) surfaces

In this section we discuss a few principal aspects of the phonon dispersion relations on the (100) surface of f.c.c. materials with a primitive unit cell as in the bulk. We first investigate the clean surface. As a matter of simplicity we consider the [110] direction, which, in the group theoretical notation of the symmetry points in the surface Brillouin-zone, is also known as the $\bar{\Gamma}\bar{X}$-direction (figure 1). For the discussion of the characteristic surface phonons of this surface

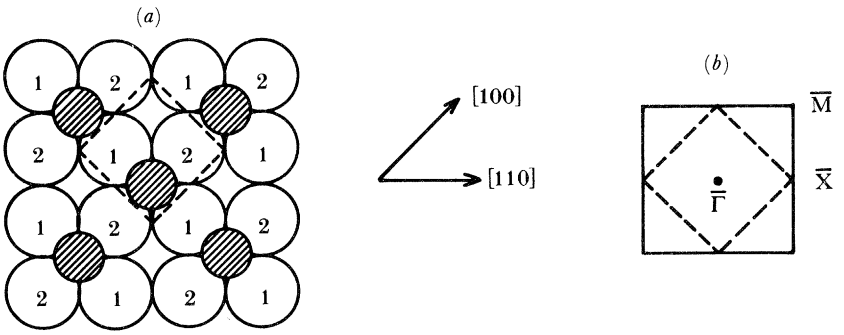

Figure 1. (*a*) (100) Surface covered with a $c(2\times2)$ overlayer. The broken lines show the unit cell for the adsorbate-covered surface. (*b*) Surface Brillouin-zone for the clean and adsorbate-covered surface (full and broken line, respectively).

it is useful to consider first the bulk phonon states projected on $\boldsymbol{Q}_{\parallel}$, the wavevector along the $\bar{\Gamma}\bar{X}$-direction. These states lie within the shaded area as plotted in figure 2. Since the sagittal plane spanned by the $\bar{\Gamma}\bar{X}$-direction and the surface normal is a mirror plane, all bulk and surface states separate into odd and even states with respect to the sagittal plane. The broken and full lines in figure 2 represent the dispersion branches of odd and even surface phonons,

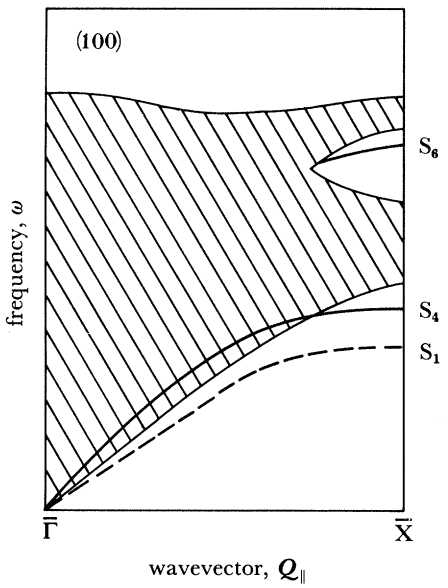

FIGURE 2. Schematic representation of the surface-phonon dispersion branches of a clean (100) surface. Broken and full lines indicate odd and even modes, respectively. For the sake of clarity surface resonances that may exist within the bulk band are not shown.

respectively. The S_4-mode (even) overlaps with the bulk states without loosing its character as a well defined surface state because the overlapping bulk states are of odd symmetry (shear transverse waves along the [110] direction). On the other hand, the mode labelled S_6 loses its localized character when the branch enters the area of bulk states. The displacement patterns of the three surface eigenmodes at $\bar{X}$ (S_1, S_4 and S_6) are plotted in figure 3. We see that S_4 is polarized strictly perpendicularly in the first layer and parallel in the second, while S_6 is polarized parallel in the first and perpendicularly in the second. A particularly interesting type of mode at $\bar{X}$ is S_1. Clearly, just the inspection of the symmetry of the problem allows one to state that for a system where the coupling of the atoms is mediated entirely by nearest-neighbour interactions, the second-layer atoms and all atoms underneath do not participate in the S_1-motion at $\bar{X}$. Therefore the S_1-mode at $\bar{X}$ depends only on the interatomic force constant between the first and second layer, and it is, in fact, straightforward to write down the frequency of that

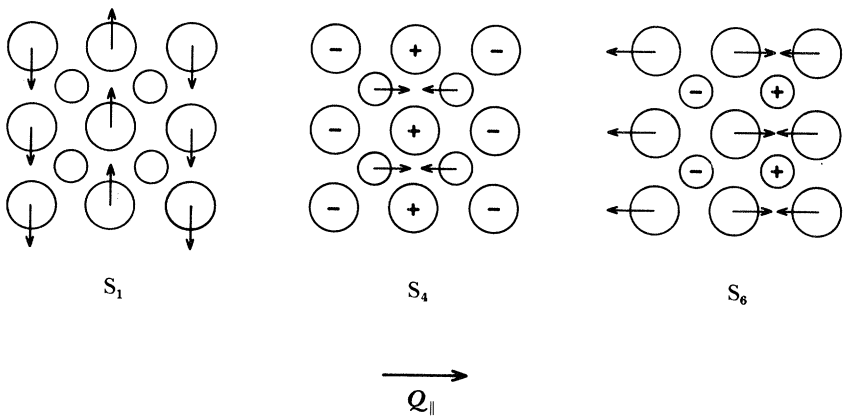

FIGURE 3. Surface phonons S_1, S_4 and S_6 at $\bar{X}$. Small circles are the atoms in the second layer.

particular mode in terms of the force constant. Assuming that the distance between the first and second layer remains as in the bulk the frequency is

$$\omega = \sqrt{k_{12}}, \tag{1}$$

with $k_{12} = \phi''_{12}/M_s$, ϕ''_{12} the second derivative of the pair potential for the coupling between the first and second layer atoms, and M_s the mass of the substrate atoms. We note that a mode localized in the second layer (S_5; Allen *et al.* (1971)) also exists if ϕ''_{12} is smaller than the force constant between bulk atoms.

Additional surface-phonon dispersion branches arise when the surface is covered with an overlayer of adatoms. Overlayers $p(2\times2)$ and $c(2\times2)$ can be prepared with oxygen, sulphur, tellurium and selenium (Somorjai 1981). With a $c(2\times2)$ overlayer the surface unit cell becomes twice as large in area and contains one adsorbate and two substrate atoms (figure 1). The plane spanned by the surface normal and the $\bar{\Gamma}\bar{X}$-direction still remains a mirror plane, but only when drawn through the adsorbate atoms. The additional adsorbate atom gives rise to three additional surface-phonon branches, two of even and one of odd symmetry. In figure 4 we present typical dispersion curves for the $c(2\times2)$ overlayer on the Ni(100) surface. At the $\bar{\Gamma}$ and the $\bar{X}$ point one odd and one even branch merge and form the degenerate parallel mode of the adsorbate. The degeneracy arises from the four-fold symmetry of the adsorption site (E-type vibration). The other surface-phonon branch along the $\bar{\Gamma}\bar{X}$-direction is perpendicularly polarized at both $\bar{\Gamma}$ and $\bar{X}$. Along the $\bar{\Gamma}\bar{X}$-direction the two even branches can mix, and a crossover of polarization character between the branches is possible as one moves from $\bar{\Gamma}$ to $\bar{X}$. In figure 4 we have drawn the two even branches well separated in frequency. In that case the polarization of the two branches will essentially remain perpendicular and parallel throughout the zone, respectively. We have also drawn the adsorbate-induced branches to lie above the bulk band of the substrate. This, of course, depends on the force constants and adsorbate masses involved.

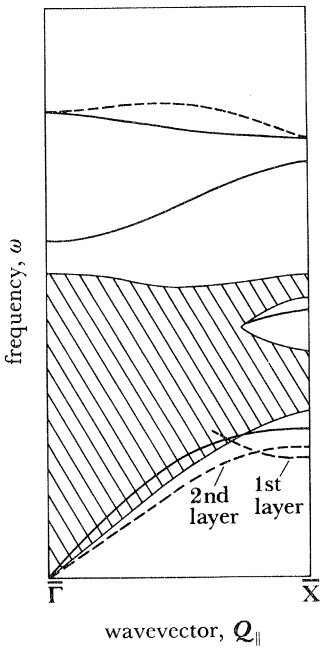

FIGURE 4. Schematic representation of surface phonons of $c(2\times2)$ on (100) surface. Broken and full lines are odd and even modes, respectively. See text for further discussion.

Let us examine the characteristics of the two clean-surface acoustic modes, namely the S_4 and S_1 surface phonons in the presence of the $c(2\times2)$ overlayer. As seen in figure 4, the S_4-mode continues to exist along the $\Gamma\bar{X}$-direction as on the clean surface with its maximum amplitude in the top substrate layer. Its frequency at the $\bar{X}$ point is determined largely by the strength of the coupling between the substrate atoms in the first and second layer and to a lesser extent by the lateral coupling between the adsorbate atoms. The clean-surface S_1-mode, which is odd with respect to reflection about the sagittal plane, however, behaves differently. This mode couples to the displacement of the adsorbate atoms that are also of odd symmetry and the coupling is such that the displacement patterns of the first-layer substrate atoms is now a linear combination of the S_1-mode at two mutually perpendicular $\bar{X}$ points. Both these linear combinations give rise to optical modes with one of them having the frequency $\sqrt{k_{12}}$ at the $\bar{X}$ point. The shear horizontal acoustic mode, which for the clean surface penetrates from the top layer all the way into the bulk, no longer exists on the top substrate layer in the presence of a $c(2\times2)$ overlayer. The substrate second layer still supports such a mode. We indicate these modes in figure 4.

With this comment we conclude the general description of the surface-phonon spectrum of (100) surfaces and turn to the experimental results and their lattice dynamical analysis.

3. Dispersion curves of Ni(100) covered with $c(2\times2)$ overlayers of sulphur and oxygen

Surface-phonon dispersion curves of clean Ni(100) surfaces and Ni(100) covered with $c(2\times2)$ overlayers of sulphur and oxygen (Rahman *et al.* 1984; Lehwald *et al.* 1985) have been studied by using inelastic scattering of low-energy electrons. The scattering plane was aligned with the [110] direction and the surface normal in the experiments. Owing to selection rules applicable to electron spectroscopy only the even modes are observable in this geometry (for a general discussion see Ibach & Mills (1982)). Both parallel and perpendicular even modes can be probed, usually at different electron energies. Experimental data were analysed with a lattice dynamical model to calculate the dispersion of the adsorbate–substrate surface modes and resonances. To keep the calculations free from too many unknown parameters, nearest-neighbour interactions between the atoms and central forces are considered. Next-neighbour and angle-bending interactions for the adsorbate atoms have been included whenever it seemed necessary to do so. Calculations were made with the aid of Fourier-transformed Green functions constructed from the atomic displacements (Rahman *et al.* 1984; Ibach & Mills 1982). The equations of motion for these Green functions give rise to a hierarchy of equations connecting the displacements of the atoms in one layer to those in the layer above and below. The equations for the adsorbate layer together with the equations for the first, second and third nickel layer, supplemented by those associated with layers deep in the bulk can be written analytically and solved by using standard methods.

Experimental results (Rahman *et al.* 1984; Lehwald *et al.* 1985) and theoretical dispersion curves are shown in figure 5*a*, *b* for the sulphur and oxygen overlayer, respectively. Parameters used for the vertical distance of the adsorbate $R_\perp$ were taken from independent structure analyses. The force constant for the adsorbate–substrate coupling ϕ''_{01} was matched to reproduce the frequency of the vertical motion of the adsorbate at $\bar{\Gamma}$. For the oxygen overlayer it was found necessary to introduce also a lateral oxygen–oxygen coupling constant ϕ''_{00}. We further

allowed the force constant between first- and second-layer nickel atoms ϕ''_{12} to be different from the bulk. This was found necessary even for the description of the clean surface where an appropriate match to experimental data (Lehwald *et al.* 1983) required this force constant to be 1.2–1.3 times the value in the bulk. As seen from figure 5, this simple force-constant model

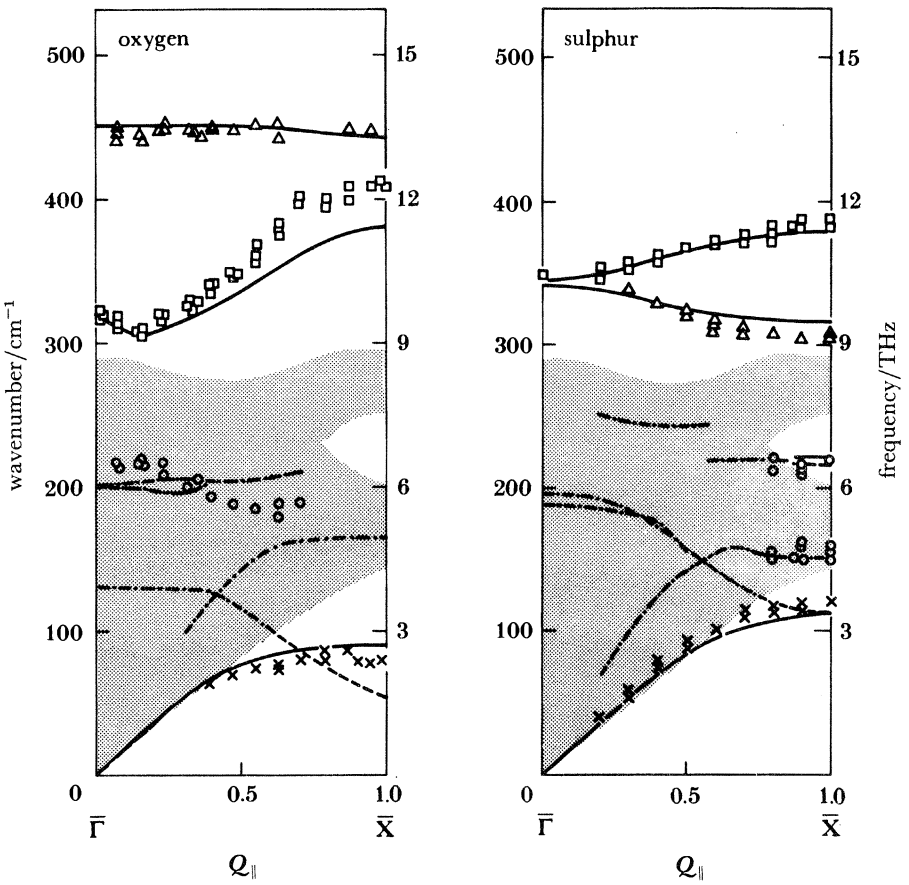

R_1/Å	0.9	1.45
ϕ''_{01}/(N cm^{-1})	0.95	0.996
k_{12}/k	0.3	1.2
l_{00}/k_{00}	0.1	0

FIGURE 5. Surface-phonon dispersion branches for Ni(100) covered with a $c(2\times2)$ overlayer of oxygen and sulphur, respectively. Only the even modes are seen experimentally. The parallel and perpendicularly polarized branch for the adsorbate modes are indicated by triangles and squares, respectively. Experimental data points for surface resonances are indicated by circles, the S_4-mode by crosses. Experimental data are from Lehwald *et al.* (1984) and Rahman *et al.* (1984). Dispersion branches are calculated from the parameters given in the table below the figure. Odd modes are shown by broken lines, resonances by chained lines.

gives an acceptable fit to the data. The two sets of dispersion curves in figure 5*a*, *b* differ, however, with respect to two features. While for the oxygen overlayer the upper and lower dispersion branches are parallel and perpendicularly polarized, respectively, the polarization is reversed for sulphur. This is essentially due to the different distance of the overlayer atoms from the surface. Another important difference is that on the sulphur-covered surface the experimental data for the S_4-mode can be matched by retaining the force constant for the coupling between first- and second-layer nickel atoms, ϕ''_{12}, at the clean-surface value, whereas

for the oxygen-covered surface ϕ''_{12} had to be reduced substantially and assumes 0.3 of the bulk value. In figure 5 we have also plotted the dispersion relation for the S_1-related mode (chained line), discussed earlier, whose frequency falls even below that of the S_4-mode and acquires the remarkably low value of *ca.* 60 cm^{-1} at $\overline{X}$ for the oxygen-covered surface.

The reduction in the force constant between the first- and second-layer nickel atoms indicates a substantial effect of the adsorbate atom on the nickel bonding. Measurements of the spacing between the first and second layer by using high-energy ion scattering (Frenken *et al.* 1983) have further shown that the softening of the S_1 and S_4 surface phonons is accompanied by an increase in the bond distance. While on the clean surface the interlayer spacing is reduced by $-3\,\%$ compared to the bulk, the spacing is enlarged by $5\,\%$ for the surface covered with a $c(2\times 2)$ oxygen overlayer.

The question of what happens when the force constant ϕ''_{12} is reduced further and approaches zero arises. To pursue that question we first consider the lattice dynamical equations for the Green functions for the modes at $\overline{X}$ on $c(2\times 2)$ covered surfaces. We will see that the assumption of $\phi''_{12}\sim 0$ makes the S_1-related mode soft, giving rise to a particular reconstruction. The predicted reconstruction is actually observed with Ni(100) surfaces covered with a $c(2\times 2)$ overlayer of carbon.

4. Soft surface-phonon reconstruction

Following earlier papers, we use the Green function

$$U_{\alpha\beta}(l_z,\kappa;\,l'_z,\kappa';\,\boldsymbol{Q}_\parallel,\omega)=\sum_s \frac{e^{(s)}_\alpha(\boldsymbol{Q}_\parallel;\,l_z,\kappa)\;e^{(s)}_\beta(\boldsymbol{q}_\parallel;\,l'_z,\kappa')^*}{\omega^2-\omega_s^2(\boldsymbol{Q}_\parallel)}, \tag{2}$$

where $e^{(s)}_\alpha(\boldsymbol{Q}_\parallel,l_z,\kappa)$ is the αth Cartesian component of the displacement of the κth atom in the unit cell in the layer l_z and $\omega_s(\boldsymbol{Q}_\parallel)$ is the frequency of the eigenmode s with the wavevector $\boldsymbol{Q}_\parallel$. The equation of motion for this Green function for the even and odd modes have been given in Rahman *et al.* (1984) and Rahman (1986), respectively.

Let us begin here by writing the equation of motion for the modes with odd symmetry, with respect to the sagittal plane, with $\boldsymbol{Q}_\parallel$ lying along the $\overline{\Gamma}\overline{X}$-direction. This will enable us to see clearly what types of substrate modes couple into the adsorbate motion. The particular function of the oxygen motion that we are interested in is defined as

$$U^-_\parallel(01;)\equiv U_{xx}(01;\,01;\,\boldsymbol{Q}_\parallel,\omega)-U_{yy}(01;\,01;\,\boldsymbol{Q}_\parallel,\omega), \tag{3}$$

which obeys the following hierarchy of equations:

$$\begin{aligned}&[\omega^2-2k'_{00}-2l_{00}(1-\cos 2aQ_x)]\,U^-_\parallel(01;)\\&\qquad+2k_{01}\cos aQ_x\,U^-_\parallel(1,21;)-2ik_{01}r_\perp\sin aQ_x\,U^-_\perp(1;)=1;\end{aligned} \tag{4}$$

$$\begin{aligned}&(\omega^2-\alpha_1-2k'_{00}-2k_{11}\cos^2 aQ_x-k_{12})\,U^-_\parallel(1,21;)\\&\qquad+2k_{01}\cos aQ_x\,U^-_\parallel(01;)-\alpha_3\cos aQ_x\,U^-_\perp(1;)+2k_{11}\cos^2 aQ_x\,U^-_\parallel(1,12;)\\&\qquad\qquad+k_{12}\cos aQ_x\,U^-_\parallel(22;)=0;\end{aligned} \tag{5}$$

$$\begin{aligned}&(\omega^2-\alpha_2-2k'_{00}r_\perp^2-2k_{12})\,U^-_\perp(1;)+2ik_{01}\sin aQ_x\,U^-_\parallel(01;)\\&\qquad+ik_{12}\sin aQ_x\,U^-_\parallel(21;)+\alpha_3\cos aQ_x\,U^-_\parallel(1,21;)-ik_{12}\sin aQ_x\,U_\parallel(22;)=0;\end{aligned} \tag{6}$$

$$(\omega^2-2k_{11}\cos^2 aQ_x-k_{12})\,U^-_\parallel(1,12;)+2k_{11}\cos^2 aQ_x\,U^-_\parallel(1,21;)+k_{12}\cos aQ_x\,U^-_\parallel(21;)=0; \tag{7}$$

$$(\omega^2-k_{12}-3k)\,U_{\parallel}^{-}(21;)+k_{12}\cos aQ_x\,U_{\parallel}^{-}(1,12;)-\mathrm{i}k_{12}\sin aQ_x\,U_{\perp}^{-}(1;)$$
$$+k\cos aQ_x\,U_{\parallel}^{-}(3,12;)+\mathrm{i}k\sin aQ_x\,U_{\perp}^{-}(3;)+2kU_{\parallel}^{-}(22;)=0; \quad (8)$$

$$(\omega^2-k_{12}-3k)\,U_{\parallel}(22;)+k_{12}\cos aQ_x\,U_{\parallel}^{-}(1,21;)+\mathrm{i}k_{12}\sin aQ_x\,U_{\perp}^{-}(1;)$$
$$+k\cos aQ_x\,U_{\parallel}^{-}(3,21;)+\mathrm{i}k\sin aQ_x\,U_{\perp}^{-}(3;)+2kU_{\parallel}^{-}(21;)=0; \quad (9)$$

and so on for equations involving the motion of the third and higher layer atoms. In the above equations we have used the definitions

$$U_{\parallel}^{-}(l_z\kappa\kappa';)\equiv U_{xx}(l_z\kappa;01;\boldsymbol{Q}_{\parallel}\omega)-U_{yy}(l_z\kappa';01;\boldsymbol{Q}_{\parallel}\omega), \quad (10)$$

$$U_{\perp}^{-}(l_z;)\equiv U_{zz}(l_z2;01;\boldsymbol{Q}_{\parallel}\omega)-U_{zz}(l_z1;01;\boldsymbol{Q}_{\parallel}\omega), \quad (11)$$

$$U_{\parallel}^{-}(l_z\kappa;)\equiv U_{xx}(l_z\kappa;01;\boldsymbol{Q}_{\parallel}\omega)-U_{yy}(l_z\kappa;01;Q_{\parallel}\omega). \quad (12)$$

Note that we have used $l_z=0$ for the adsorbate layer and $l_z=1$ for the first substrate layer and so on. The force constants that enter have the form

$$k_{00}=\phi''_{01}/M_{\mathrm{a}}(1+r_{\perp}^2),\quad k'_{00}=\phi''_{01}/M_{\mathrm{s}}(1+r_{\perp}^2),$$
$$k_{01}=\phi''_{01}/(M_{\mathrm{a}}M_{\mathrm{s}})^{\frac{1}{2}}(1+r_{\perp}^2),\quad k_{12}=\phi''_{12}/M_{\mathrm{s}},\quad k_{11}=\phi''_{11}/M_{\mathrm{s}},$$
$$k=\phi''/M_{\mathrm{s}},\quad l_{00}=\phi''_{00}/M_{\mathrm{a}},$$

where $\phi''_{l_zl'_z}$ is the second derivative of the pair potential between atoms in layer l_z and l'_z, $r_{\perp}$ is equal to $R_{\perp}/a$ with $a=a_0/\sqrt{2}$, such that $R_{\perp}$ is the vertical height at which the adsorbate atoms sit above the substrate plane and a_0 is the nearest-neighbour distance, and M_{a} and M_{s} are the masses of the adsorbate and substrate atoms, respectively. The force constants α_1, α_2 and α_3 refer to angle-bending interactions between adsorbate atoms and their nearest neighbours, as discussed in Rahman *et al.* (1984).

It is worth pointing out that the displacement pattern ensuing from the Green function combination $U_{\parallel}^{-}(1,12;)$ and $U_{\parallel}^{-}(1,21;)$ are indeed related to the S_1-mode for the clean-metal surface. In fact they are, respectively, the symmetric and antisymmetric linear combinations of the S_1-mode at the two mutually orthogonal $\overline{\mathrm{X}}$ points.

It follows directly from (4)–(9) that at the $\overline{\mathrm{X}}$ point, where $Q_x=\pi/2a$, the modes $U_{\parallel}^{-}(1,12;)$ and $U_{\parallel}^{-}(1,21;)$ are decoupled from the others and have the simple form

$$U_{\parallel}^{-}(1,12;)=1/(\omega^2-2k_{12}) \quad (13)$$

and

$$U_{\parallel}^{-}(1,21;)=1/(\omega^2-2k'_{00}-k_{12}-\alpha_1). \quad (14)$$

The mode $U_{\parallel}^{-}(1,12;)$ thus becomes soft at $\overline{\mathrm{X}}$ when k_{12} approaches zero, while the mode $U_{\parallel}^{-}(1,21;)$, although decoupled from the other modes, maintains a finite frequency. In figure 6*c*, *d*, we show the displacement patterns arising from modes $U_{\parallel}^{-}(1,12;)$ and $U_{\parallel}^{-}(1,21;)$ at the $\overline{\mathrm{X}}$ point. If we now compare the two proposed reconstruction patterns for the Ni(100) surface-layer atoms in the presence of a $c(2\times2)$ overlayer of carbon, as shown in figure 6*a*, *b*, with these displacement patterns, in light of the discussion above regarding the softening of the mode, we see that the pattern in figure 6*a* is preferred.

The reconstruction as shown in figure 6*a* is also favoured by a dynamical analysis of the l.e.e.d. intensities. We have thus established a connection between the carbon-induced reconstruction of the surface and the softening of a particular force constant.

PHILOSOPHICAL TRANSACTIONS OF THE ROYAL SOCIETY A MATHEMATICAL, PHYSICAL & ENGINEERING SCIENCES

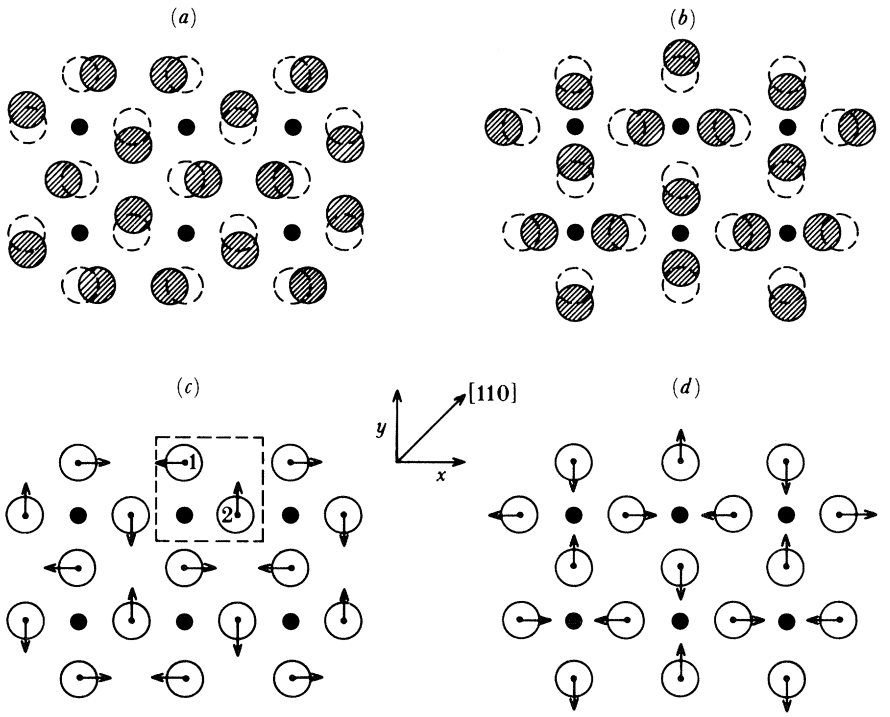

FIGURE 6. Proposed reconstruction pattern for the Ni(100) surface covered with a $c(2\times2)$ overlayer of carbon ((*a*) and (*b*)). The pattern displayed in (*a*) is preferred by a dynamical analysis of the l.e.e.d. intensities (Onuferko 1979). (*c*), (*d*) Displacement pattern of the $U_{\parallel}^{-}(1,12;)$ and the $U^{-}(1,21;)$ modes, respectively. The $U_{\parallel}^{-}(1,12;)$ mode becomes soft as k_{12} approaches zero.

While the result has been derived in a nearest-neighbour central-force model it can easily be seen that the result applies also to a more general force field with angle-bending forces on the adsorbate atom and central-forces between the adsorbate atoms or between the adsorbate atoms and the second-layer substrate atoms. This is because the adsorbate does not participate in the $U_{\parallel}^{-}(1,21;)$ motion.

Let us now consider the modes at the $\overline{\mathrm{X}}$ point that are even under reflection with respect to the sagittal plane, to see if any mode there becomes soft as k_{12} tends to zero. For our purpose here it is sufficient to put $k_{12}=0$ in the equation for these modes, as given in Rahman *et al.* (1984). Here we have two sets of simple equations, one with the vertical motion of the adsorbates coupling to the parallel motion of the top layer substrate atoms, and the other with just the opposite. The equations that determine the parallel motion of the substrate atoms are

$$(\omega^2-\alpha_1-2k'_{00}-4k_{11})\,U_{\parallel}^{+}(1,21;)+\mathrm{i}(4k_{01}r_{\perp}+2\alpha_4)\,U_{z\beta}(01;)=1, \tag{15}$$

$$(\omega^2-4k_{00}r_{\perp}^2-\alpha)\,U_{z\beta}(01;)-\mathrm{i}(2k_{01}r_{\perp}+\alpha_4)\,U_{\parallel}^{+}(1,21;)=0. \tag{16}$$

In a similar way to the modes with odd symmetry, we have used the definitions

$$U_{\parallel}^{+}(1,21;)\equiv U_{xx}(12;01;\boldsymbol{Q}_{\parallel}\omega)+U_{yy}(11;01;\boldsymbol{Q}_{\parallel}\omega), \tag{17}$$

$$U_{z\beta}(01;)\equiv U_{zx}(01;01;\boldsymbol{Q}_{\parallel}\omega)+U_{zy}(01;01;\boldsymbol{Q}_{\parallel}\omega). \tag{18}$$

Clearly the frequency of $U_{\parallel}^{+}(1,21;)$, whose displacement pattern is that of the symmetric combination of that of the S_6 surface phonon, remains at a finite frequency when $k_{12}=0$.

The equation for the perpendicular motion of the substrate atoms, at the $\overline{\mathrm{X}}$ point, are also very simple. Thus

$$(\omega^2 - 2k'_{00}\, r_\perp^2)\, U^{\mathrm{L}}(1;) + 2ik_{01}\, r_\perp\, U_\parallel^+(01;) = 1, \tag{19}$$

$$-2ik_{01}\, r_\perp\, U^{\mathrm{L}}(1;) + (\omega^2 - 4l_{00} - 2k_{00})\, U_\parallel^+(01;) = 0, \tag{20}$$

where

$$U^{\mathrm{L}}(1;) = U_{zz}(11;01;\boldsymbol{Q}_\parallel\,\omega) + U_{zz}(12;01;\boldsymbol{Q}_\parallel\,\omega), \tag{21}$$

$$U_\parallel^+(01;) = U_{xz}(01;01;\boldsymbol{Q}_\parallel\,\omega) + U_{yz}(01;01;\boldsymbol{Q}_\parallel\,\omega). \tag{22}$$

Equations (19) and (20) are easily solved to give

$$U^{\mathrm{L}}(1;) = \frac{\omega^2 - 2k_{00} - 4l_{00}}{(\omega^2 - 2k'_{00}\, r_\perp^2)\,(\omega^2 - 2k_{00} - 4l_{00}) - 4k_{01}^2\, r_\perp^2}. \tag{23}$$

The displacement pattern associated with the $U^{\mathrm{L}}(1;)$ mode is identical to that of the clean-surface S_4-mode shown in figure 3. It is clear that provided $l_{00} \neq 0$, the S_4-mode has a finite frequency, even when $k_{12} = 0$. The argument may be made that for a number of adsorbates, l_{00} or the adsorbate–adsorbate interaction is negligible, consequently when k_{12} becomes zero or negative the S_4 surface phonon will also freeze and cause a lateral reconstruction of the surface. This may indeed happen, but what is of interest here is the horizontal reconstruction that has been observed with a carbon overlayer on Ni(100).

We have seen from the above that the freezing of a particular surface phonon was compatible with one of the proposed reconstruction patterns, which leads to the conclusion that the reconstruction was driven by the softening of a surface phonon. For the sake of completeness we need to show that no other mode with displacement patterns parallel to the surface undergoes such a softening when $k_{12} = 0$. Such a possibility can exist only at $\overline{\mathrm{M}}$, the other high-symmetry point, where the parallel motion of the adsorbate atoms couples to the parallel motion of the substrate atoms. Once again when $k_{12} = 0$ it is easy to see (following Rahman *et al.* 1984) that the equations at the $\overline{\mathrm{M}}$ point for the pertinent modes form two sets, each relating to a particular type of motion of the adsorbate. Thus

$$(\omega^2 - 2k'_{00} - 2k_{11})\, U_\parallel(1,21;) - 2k_{01}\, U_\parallel^+(01;) - 2k_{11}\, U_\parallel^-(1,12;) = 1, \tag{24}$$

$$(\omega^2 - 2k_{00})\, U_\parallel^+(01;) - 2k_{01}\, U_\parallel^-(1,21;) = 0, \tag{25}$$

$$(\omega^2 - 2k_{11})\, U_\parallel^-(1,12;) - 2k_{11}\, U_\parallel^-(1,21;) = 0, \tag{26}$$

and an equivalent set of coupled equations for the other parallel modes is represented by

$$(\omega^2 - 2k'_{00} - 2k_{11})\, U_\parallel^+(1,21;) - 2k_{01}\, U_\parallel^-(01;) - 2k_{11}\, U_\parallel^+(1,12;) = 1, \tag{27}$$

$$(\omega^2 - 2k_{00})\, U_\parallel^-(01;) - 2k_{01}\, U_\parallel^+(1,21;) = 0, \tag{28}$$

$$(\omega^2 - 2k_{11})\, U_\parallel^+(1,12;) - 2k_{11}\, U_\parallel^+(1,21;) = 0. \tag{29}$$

Neither set of equations yields a mode with zero frequency. We are, therefore, justified in stating that when $k_{12} = 0$ the only mode that goes soft is $U_\parallel^-(1,12)$.

To summarize, we have shown that the assumption of k_{12} becoming vanishingly small leads to a particular reconstruction and that this reconstruction is the one observed with a $c(2\times 2)$ overlayer of carbon on Ni(100). We have further seen that the assumption of k_{12} becoming vanishingly small is not unreasonable since k_{12} becomes already small with an overlayer of

oxygen. If one considers the sequence S, O, and C, the carbon atom has the highest binding energy with nickel. The carbon atom also sits closest to the surface with a vertical distance of *ca.* 0.1 Å† (Onuferko *et al.* 1979). While the connection between $k_{12} \leqslant 0$ and the reconstruction is established, it is not clear yet what makes k_{12} to become zero or negative. One possibility would be that the increased bonding between the adsorbate and the substrate reduces the backbonding of the first substrate layer to the required extent. We will see, however, that the total energy calculation to be described in the following provides another lucid and more reasonable interpretation.

5. Total energy calculations

In this section we consider the problem of adsorbate-induced reconstructions from a localized point of view. We study the chemisorption of a single carbon and oxygen atom on a (100) metal surface and simulate the local environment of the adatom by using the atomic cluster shown in figure 7. The surface is represented by two layers of metal atoms separated by a distance d, which are allowed to relax independently (variables a_1 and a_2) and to rotate with respect to one another (angle α). The numerical results presented below will be specific for an aluminium surface; the qualitative conclusions, however, will be of general validity and should be also applicable to the Ni surface discussed above. For the energy calculation we use the Hohenberg–Kohn–Sham (H.K.S.) scheme with a localized muffin-tin orbital basis (Miller *et al.* 1983). In the present study we included s, p and d functions in all sites.

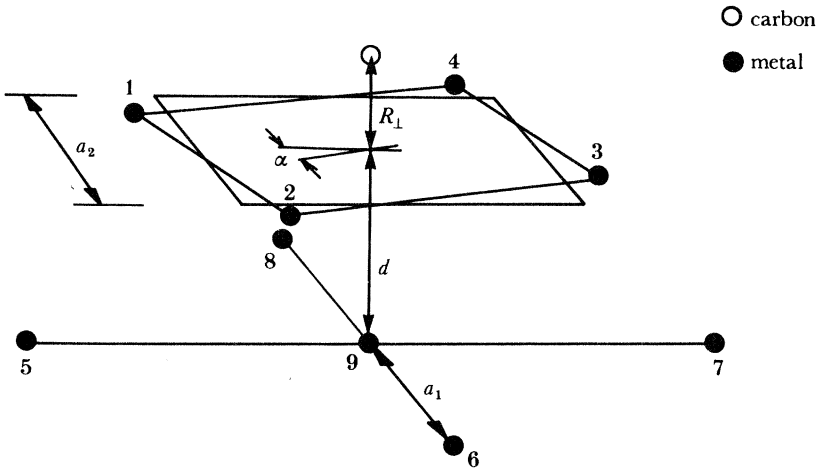

Figure 7. The geometry of the Al_9 cluster with an adsorbed carbon atom.

Figures 8 and 9 show the variation of the binding energy E_b and cluster dipole as a function of the distance $R_\perp$ between the adatom and the surface for oxygen and carbon, respectively. In these curves the distances between the metal atoms have been kept fixed and equal to the aluminium bulk values. For oxygen, it may be worth noticing that the cluster dipole indicates a charge transfer *to* the surface. This shows that a decrease in the work function does not imply that the O atom lies under the top layer, as often assumed (den Boer *et al.* 1980; Erskine & Strong 1982). We also point out the flatness of the binding energy curve, which means a large

† 1 Å = 10^{-10} m = 0.1 nm.

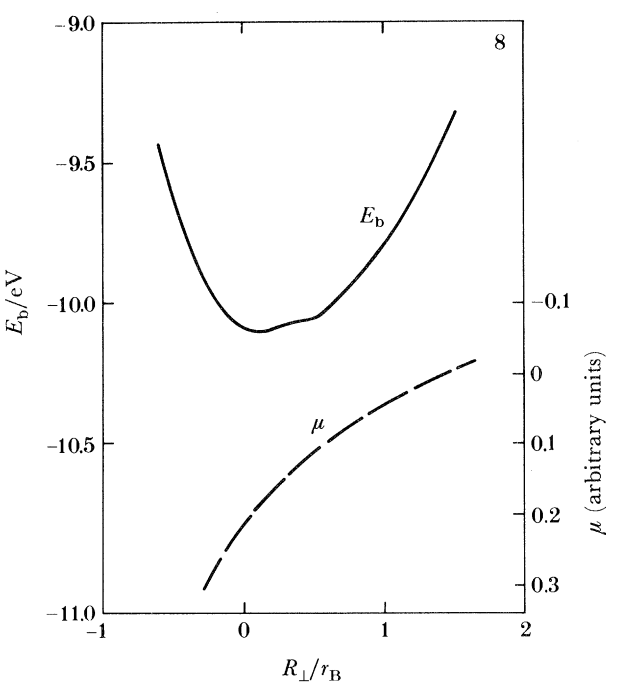

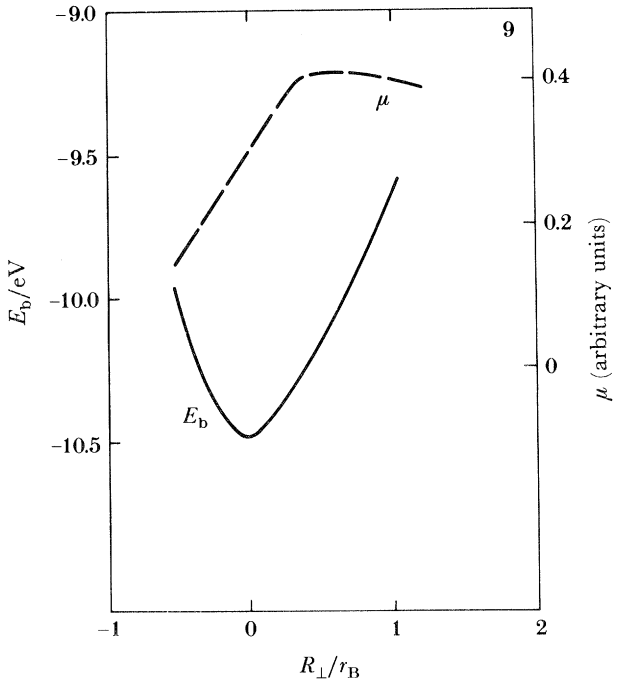

FIGURE 8. Variation of the binding energy E_b and total dipole moment of the cluster as a function of the distance $R_\perp$ of the oxygen atom from the surface. Metal atom distances are kept fixed at the value for bulk aluminium.

FIGURE 9. Variation of the binding energy E_b and the dipole moment for an adsorbed carbon atom.

zero-point motion of the O atom and a possible break down of the harmonic theory. The H.K.S. binding energy $E_b = 10.1$ eV is larger than the Hartree–Fock energy (*ca.* 5 eV) (see Batra & Kleinman 1984), as is usually the case, with the experimental value lying somewhere between both values. For carbon, no total energy calculations have been reported, to the best of our knowledge. We find a binding energy of 10.5 eV.

The large binding energies mean that the Al–O and Al–C interactions are stronger than the Al–Al interaction, so that the reconstruction of the surface is expected to play an important role in the chemisorption process. If we let the cluster relax we find the equilibrium geometry for the Al_9 and Al_9–C clusters displayed in table 1. The Al_9 contracts uniformly about 10% in its linear dimensions: because of the finite size of the cluster the electron charge is not completely confined between the atoms, resulting in a reduced kinetic-energy repulsion. Upon adsorption of a C atom the separation between the metal layers increases by *ca.* 3% and the distances in the top layer expand by about 10%. The latter expansion results from the attraction of the C atom to the second metal layer, which gives rise to a repulsive interaction with the atoms of the top layer. The increased separation between the metal layers shows a reduced Al–Al interaction. Distortions with finite rotation angle α have been found to be energetically unfavourable for the relaxed cluster.

TABLE 1. EQUILIBRIUM GEOMETRY FOR Al, AND Al_9–C CLUSTERS

	a_1/r_B	a_2/R_B	d/r_B	$R_\perp/r_B$	α/deg
unrelaxed Al_9–C	5.40	5.40	3.82	0.0	0.0
relaxed Al_9	5.00	5.00	3.44	—	0.0
relaxed Al_9–C	5.00	5.40	3.54	0.2	0.0

PHILOSOPHICAL TRANSACTIONS OF THE ROYAL SOCIETY A MATHEMATICAL, PHYSICAL & ENGINEERING SCIENCES

The observed surface reconstruction for carbon on Ni(100) corresponds to a finite rotation α between the metal layers of our Al_9 cluster. In the following we shall address the question: under which circumstances is such a rotational construction energetically favourable? To that end it is convenient to think of the net force on a specific atom as a superposition of pair interactions with all the remaining atoms of the system. In this approximation we shall be able to interpret the reconstruction as a result of strains in the interaction between specific pairs of atoms. We consider two types of rotational reconstruction.

(*a*) *Rotational reconstruction for an extended surface*

We mentioned above that chemisorption of carbon on a finite aluminium cluster gives rise to a repulsion of the metal atoms of the top layer. We expect this result to be valid as well for low coverage (under 25 %) on an extended surface. For a $p(2\times2)$ structure, for instance, this repulsion should lead to a surface reconstruction of the form shown in figure 10*a*. For

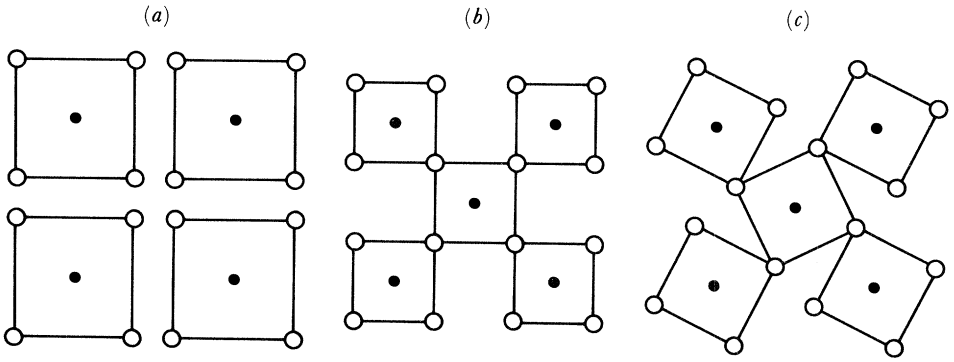

FIGURE 10. Possible surface reconstruction patterns for (2×2) overlayer which can result from an adsorbate-induced compression within the first layer. For a $p(2\times2)$ overlayer the comparison would lead to a sideways shift (*a*) of the substrate atoms. The compressional forces on the surface substrate atoms are balanced when the surface is covered with a $c(2\times2)$ overlayer (*b*). If, however, the compression becomes too large the unreconstructed surface could become unstable and a rotational pattern forms (*c*).

coverage larger than 25 % such a reconstruction is no longer possible and symmetry may force the structure illustrated in figure 10*b*. This structure necessarily implies internal stresses on the surface. The Al–Al interaction tends to preserve the four-fold symmetry, while the repulsion between the C and Al atoms tends to favour a surface distortion of the form shown in figure 10*c*. Depending on the relative strength of these two competing effects we should find different behaviours. If the interaction between the adatom and the metal atoms dominates a surface reconstruction should occur. This could be the example of carbon on Ni(100). If the metal–metal interaction dominates we expect a softening of the δ_4 phonon mode, as observed for oxygen on Ni(100).

(*b*) *Rotational reconstruction in the finite cluster*

Figure 11 shows the variation of the energy as a function of the rotation angle α, for various positions of the C atom. The separation α between the metal layers has been allowed to relax, but all the other parameters have been kept constant. With increasing distance of the C atom under the top layer the rotation softens gradually, until for $R_\perp \simeq -0.8\,r_B$ (where r_B is the Bohr radius of a distortion with $\alpha = 10°$ becomes energetically favourable. The origin of the distortion is schematically illustrated in the inset of figure 11. The C atom induces an increased

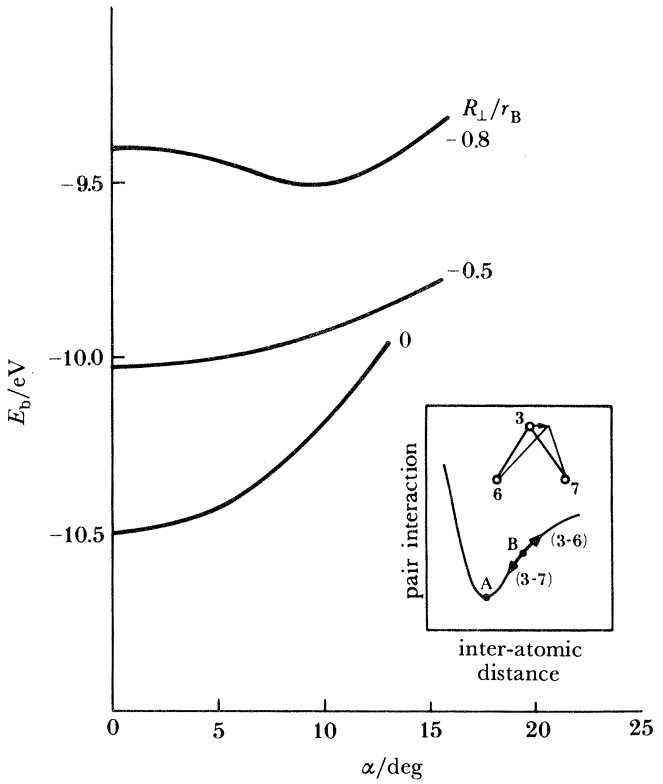

FIGURE 11. Variation of the binding energy as a function of rotation angle α. If the carbon atom is pushed inside the cluster (which requires energy) The unrotated cluster becomes unstable with respect to rotation. The inset provides an explanation for this effect in terms of the pair potential between the Al atom of the first and second layer (see text).

separation between the metal layers, so that the interaction between them becomes attractive (point B in the pair potential). Under a rotation α an atom of the top layer, say atom number 3, gains some energy by moving closer to atom number 7 and loses some by moving away from atom number 6. If the separation between the layers is large enough that B lies at or beyond the inflexion point of the pair-interaction curve, i.e. $E(3\text{–}7)+E(3\text{–}6) \leqslant 0$, and the distortion becomes energetically favourable.

For the carbon on Ni(100) there is no experimental evidence that the C atom lies under the top layer. This, however, is not a necessary condition for a rotational reconstruction of this type. For instance, the bare Al_9 cluster shows the same effect when the separation between the layers is increased beyond the inflexion point of the pair interaction between the two layers, as suggested by the vibrational analysis of §4.

6. Conclusion

Our analysis of the reconstruction mechanism invoked in the carbon-covered Ni(100) surface has provided us with two models. In §4 we have seen that assuming that the second derivative for the pair potential between first- and second-layer atoms becomes negative for the unreconstructed carbon-covered nickel surface causes the rotational distortion observed experimentally. The total energy calculations have pointed out the physical origin of the effect,

namely that internal strains with an attractive interaction between the adsorbate atom and the first-layer metal atoms and a repulsive interaction between the adsorbate atom and the second-layer metal may strain the metal–metal bonds between first- and second-layer metal atoms beyond the point of inflexion for the pair potential between these atoms. Our total energy calculations on the Al_9-cluster, however, suggest that the internal strain are just opposite in sign, namely repulsive between the adsorbate atoms and the first-layer metal atom and attractive with metal atom underneath. In this case one would expect ϕ''_{12} to increase rather than decrease. Nevertheless we have shown qualitatively that the compression in the first layer may likewise cause the rotational instability. We note, however, that our cluster calculations have been made only with aluminium so far. Quantitative aspects may, therefore, not apply to nickel. Up to this point the lattice dynamical analysis has been made only with pair potentials that are at equilibrium individually. A study of the lattice dynamics of the nickel-adsorbate system including second-neighbour interactions, where the first derivatives are non-zero is required for a further analysis of the problem. The model could be tested with the experimental dispersion curves for the various adsorbates and may help to distinguish between the two alternative models.

The authors acknowledge helpful discussion with S. Lehwald and M. Rocca. J.E.M. acknowledges contributions from O. Gunnarsson, J. Harris, R. O. Jones and G. Painter to the cluster program. The work of T. S. Rahman was partly supported by the National Science Foundation under contract no. DMR-8402850. We also acknowledge travel support from NATO research grant no. 075/84.

References

Allen, R. E., Alldredge, G. P. & de Wette, F. W. 1971 *Phys. Rev.* B **4**, 1661.
Batra, I. P. & Kleinman, L. 1984 *J. Electron Spectrosc. Rel. Phen.* **33**, 175.
den Boer, M. L., Einstein, T. L., Elam, W. T., Park, R. L., Roelofs, L. D. & Laramore, G. E. 1980 *Phys. Rev. Lett.* **44**, 496.
Cunningham, S. & Trollinger, S. E. 1978 *Phys. Rev.* B **18**, 1898.
Erskine, J. L. & Strong, R. L. 1982 *Phys. Rev.* B **25**, 5547.
Farnsworth, H. E., Schlier, R. E., George, T. H. & Burger, R. M. 1958 *J. appl. Phys.* **29**, 1150.
Fasolino, A., Santoro, G. & Tosatti, E. 1980 *Phys. Rev. Lett.* **44**, 1684.
Frenken, J. W. M., van der Veen, J. E. & Allan, G. 1983 *Phys. Rev. Lett.* **51**, 1876.
Ibach, H. & Mills, D. L. 1982 *Electron energy loss spectroscopy and surface vibrations*, p. 116. New York: Academic Press.
Lehwald, S., Rocca, M., Ibach, H. & Rahman, T. S. 1985 *Phys. Rev.* (In the press.)
Lehwald, S., Szeftel, J., Ibach, H., Rahman, T. S. & Mills, D. L. 1983 *Phys. Rev. Lett.* **50**, 518.
Müller, J. E., Jones, R. O. & Harris, J. 1983 *J. chem. Phys.* **79**, 1874.
Onuferko, J. H., Woodruff, D. P. & Holland, B. W. 1979 *Surf. Sci.* **87**, 357.
Rahman, T. S. 1986 (In preparation.)
Rahman, T. S., Mills, D. L., Black, J. E., Szeftel, J. M., Lehwald, S. & Ibach, H. 1984 *Phys. Rev.* B **30**, 589.
Rocca, M., Lehwald, S., Ibach, H. & Rahman, T. S. 1984 *Surf. Sci.* **138**, L123.
Somorjai, G. A. 1981 *Chemistry in two dimensions*, p. 126. Cornell University Press.

Discussion

M. W. Roberts (*Department of Chemistry, University College, Cardiff, U.K.*). I was particularly interested in Professor Ibach's remark that in the Ni(100)–O system 'NiO' structures were observed more obviously if oxygen interaction was effected at low temperature and the adlayer warmed to 295 K. These are also the conditions for enhancing the Ni^{2+} and Ni^{3+} states revealed

in the Ni(2p) difference spectra. Are these the conditions where the influence of phonon interactions would be most significant?

H. IBACH. We have indeed found consistently that exposure of the Ni(100) surface to moderate doses of oxygen (*ca.* 10 L) at low temperatures (*ca.* 150 K) leads to the formation of NiO clusters when the crystal was subsequently annealed, while exposure at room temperature would not cause the same effect (provided the crystal had not too many defects). We attribute this effect to a softening of the nickel bonding between first- and second-layer nickel atoms when oxygen atoms occupy nearest-neighbour fourfold sites. Occupation of nearest-neighbour sites at room temperature is prevented because there oxygen diffuses sufficiently rapidly and locally forms immediately 2×2 or $c(2 \times 2)$ islands where every other site is empty. For the $c(2 \times 2)$ overlayer we see a drastic weakening of the nickel bonds from phonon dispersion curves, but not to the extent that the lattice becomes unstable.

PHILOSOPHICAL TRANSACTIONS OF THE ROYAL SOCIETY A MATHEMATICAL, PHYSICAL & ENGINEERING SCIENCES